Lab on a Chip

Capacitive Sensing of Triglyceride Film Reactions: A Proof-of-Concept Demonstration for Sensing in Simulated Duodenal Contents with Gastrointestinal Targeting Capsule System

Journal:	*Lab on a Chip*
Manuscript ID	LC-ART-02-2020-000133.R1
Article Type:	Paper
Date Submitted by the Author:	19-Apr-2020
Complete List of Authors:	Banis, George; University of Maryland at College Park, Bioengineering Beardslee, Luke; University of Maryland at College Park, Institute for Systems Research Stine, Justin; University of Maryland at College Park, Electrical and Computer Engineering Sathyam, Rajendra Mayavan; University of Maryland at College Park, Electrical and Computer Engineering Ghodssi, Reza; University of Maryland at College Park, Institute for Systems Research

Lab on a chip

Capacitive Sensing of Triglyceride Film Reactions: A Proof-of-Concept Demonstration for Sensing in Simulated Duodenal Contents with Gastrointestinal Targeting Capsule System

Authors:
George E. Banis[1,2], Luke A. Beardslee[1], Justin M. Stine[1,3], Rajendra Mayavan Sathyam[1,3], and Reza Ghodssi[1-3*]
Affiliations:
[1]Institute for Systems Research, [2]Fischell Department of Bioengineering
[3]Department of Electrical and Computer Engineering, University of Maryland, College Park, MD, USA

Abstract

Ingestible capsule systems continue to evolve to overcome drawbacks associated with traditional gastrointestinal (GI) diagnostic and therapeutic processes, such as limitations on which sections of the GI tract can be accessed or the inability to measure local biomarker concentrations. We report an integrated capsule sensing system, utilizing a hybrid packaging scheme coupled with triglyceride film-coated capacitive sensors, for measuring biochemical species present in the duodenum, such as pancreatic lipase and bile acids. The system uses microfabricated capacitive sensors interfaced with a Bluetooth Low-Energy (BLE)- microcontroller, allowing wireless connectivity to a mobile app. The triglyceride films insulate the sensor surface and react either with 0.01-1 mM lipase via hydrolysis or 0.07-7 %w/v bile acids via emulsification in simulated fluids, leading to measurable changes in capacitance. Cross reactivity of the triglyceride films is evaluated in both phosphate buffered saline (PBS) as well as pancreatic trypsin solutions. The film morphology is observed after exposure to each stimulus to better understand how these changes alter the sensor capacitance. The capsule utilizes a 3D-printed package coated with polymers that remain intact in acid solution (mimicking gastric conditions), then dissolve at a duodenum-mimicking neutral pH for triggered opening of the sensing chamber from which we can subsequently detect the presence of pancreatic lipase. This device strategy represents a significant step towards using embedded packaging and triglyceride-based materials to target specific regions of the GI tract and sensing biochemical contents for evaluating gastrointestinal health.

Keywords: Ingestible systems, capsule, capacitive sensing, system integration, gastrointestinal tract.

Introduction

Ingestible capsule systems capable of navigating the gastrointestinal (GI) tract are being developed to non-invasively address a myriad of clinical applications (1–4). The most recognizable device is the capsule endoscope, such as the PillCam (Medtronic, Dublin, Ireland), EndoCapsule (Olympus, Tokyo, Japan), and MiroCam (IntroMedic Co., Seoul, South Korea), which can visualize the entire GI tract length, but are most useful for imaging the small intestine where access via traditional

endoscopic techniques remains limited (5–8). Capsules directed toward monitoring specific GI analytes have been developed to provide more specific diagnostic information than is available with video imaging. For example, a capsule containing sensors targeting various gases, specifically H_2, CH_4, and CO_2, has been demonstrated for profiling gas content within porcine and human GI tracts and to the effects of various stimuli such as heat stress, anti-inflammatory agents, high- and low-fiber diets (9–12). There are also capsules measuring a variety of parameters including: pH, temperature, or pressure, as well as cancer markers using near-infrared sensors to measure fluorescently tagged antibodies. Integrated capsule systems have also been designed that enhance drug delivery through programmable control systems or controlled release (13,14). Several capsules have been developed to detect GI bleeding using either fluorometric sensors to measure circulating fluorophores or photodetectors measuring heme-triggered light emitted from engineered bacteria (15–19). Though they are measuring similar contents, the electronic architecture – based on their respective transduction mechanisms – and materials chosen vary, requiring differences in fabrication and integration strategies (20). For the GI bleeding capsules, one requires intravenous application of the fluorophores while the other utilizes embedded bacteria. In comparing the gas- or pH-detecting capsules, the phase or state of the detected medium varies, demanding transducers adaptable for measuring contents whether they are in gas or liquid form, both of which are present in the GI environment (21).

Recent advances in fabrication methods allowing the integration of a broader range of materials have fostered the development of more capsule devices. 3D-printing, one of the most ubiquitous and continuously expanding manufacturing technologies, has improved the time, cost efficiency, and allowable structural complexity for device prototyping compared to traditional subtractive manufacturing processes (22). Increased spatial resolution enables 3D-printing of microfluidics and microsystems packaging, while research for 3D-printed biocompatible materials has led to implementation into medical and pharmaceutical devices (22–26). Further, food-based materials, including varieties of gelatin, starches, or oils, are increasingly becoming utilized for edible electronic systems (27–30). Integration of these materials on sensors, either as electrodes or as electrode-functionalized substrates, have allowed for catalyzing reactions directly with target analytes; however, fabrication and integration challenges vary significantly, depending on the chemical composition of the material, and have yet to find utility in capsule devices (31).

This paper presents an integrated capsule system that utilizes biocompatible and biodegradable materials as packaging for GI-targeted fluid sampling, and triglyceride films for sensing digestive enzymes in a target region. Polymers that dissolve in a specific pH range are used as the packaging materials and are able to target fluids with characteristics simulating pancreatic secretions due to their characteristic pH. The pH gradient of the GI tract is relatively well understood, with the gastric – or stomach – environment known to be highly acidic (pH 1-3) (32), though can occasionally increase outside this range with different feeding or fasting states (33). Gastric secretions flowing into the duodenum are then neutralized by bicarbonate secretions entering via the sphincter of Oddi from the pancreas (pH 5-7). Therefore, systems and sensors entering the stomach must be well protected to remain stable upon entry into the small intestine. A previously developed packaging strategy is utilized in which biodegradable polymers, such as various Eudragit formulations, allow fluid to enter the capsule at specific locations within the GI tract (34). The Eudragit L100 formulation is pH-specific and dissolves above pH 6.0 but remains stable in lower pH levels, protecting the sensing chamber until the capsule reaches the duodenum (35–37). A target molecule of interest is pancreatic lipase (PL), which is known to diminish in response to a variety of pancreatic pathologies such as exocrine pancreatic insufficiency, cystic fibrosis, pancreatitis, and even pancreatic cancer (38–42). Current methods for elaborating PL activity consist of blood, urine, or stool tests, which generally require admission to a hospital or clinic, potential blood withdrawal, and

lab analysis (43). A user-friendly device capable of point-of-care (POC) PL measurements would reduce the time to reach diagnosis measurements and cost for patients suffering from chronic pancreatic conditions, which require frequent sampling and analysis (44). Lipase serves additionally as a model target – for more specific enzymes or other biomolecules that are present only in specific regions of the GI tract – for detection with the targeting capsule system presented here .

Here, stearin was used as a model substrate for measuring PL activity in a capacitive-sensing capsule system that is designed to specifically sample pancreatic secretions in the duodenum. The attractive nature of the sensors is their utility for measuring film solubility in a capsule package, which can be applied to a variety of targets analytes that induce film- or substrate-dissolving reactions. A similar sensing strategy for measuring pancreatic trypsin with films made from gelatin is previously reported (28). Testing of the sensors consisted of observing the sensor response over time frames similar to those expected while traveling through the duodenum, while immersed in varying concentrations of pancreatic lipase in a benchtop environment that reflect a similar expected range with appropriate pH.

In using this strategy, the impact of bile acids (BA) were investigated, as they were identified as a probable interfering species. BAs are synthesized from cholesterol by hepatocytes; they are shown to be elevated in GI secretions during BA malabsorption and can be further related to conditions such as irritable bowel syndrome-associated diarrhea and colorectal cancer (45–47). Because of their amphipathic nature, BAs such as cholic and deoxycholic acid act as natural detergents that emulsify triglycerides to form micelles through intercalation, aiding their digestion by PL into absorbable monoglycerides and fatty acids (48). The system was characterized by testing stearin films with BAs to determine potential nonspecific impacts and how it may affect sensing of PL, then further characterize its integration into a capsule platform with the downstream goal of wirelessly transmitting metrics of these biochemical species to a patient for potential clinical evaluation.

Figure 1 illustrates the prospective data flow from the capsule sensor to the patient's physician. The system is potentially low-cost, biocompatible, and easily interfaces with a mobile phone for wirelessly collecting data via Bluetooth Low Energy (BLE) The system offers promise for further development of ingestible diagnostic systems that would benefit from novel integration and packaging strategies for measuring biomarkers, such as enzymes, in GI secretions.

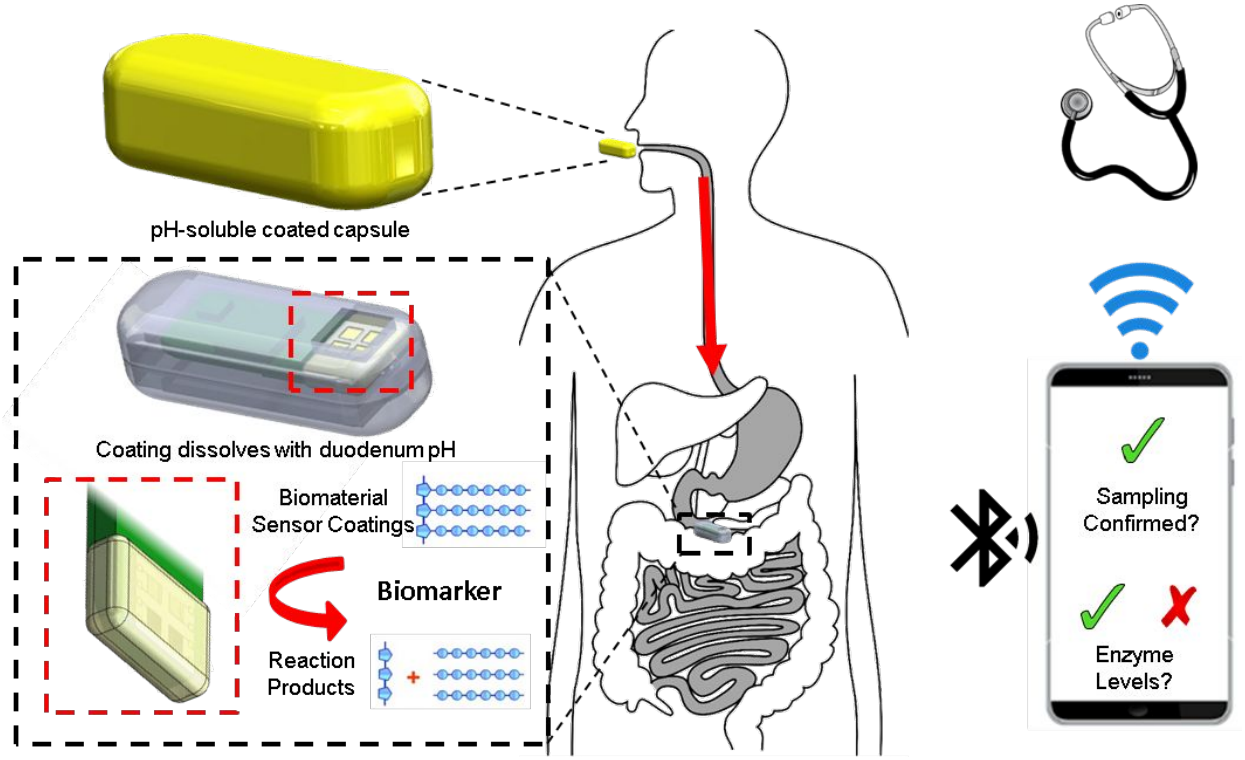

Figure 1: Depiction of application. The pH-soluble coated capsule is ingested and protected from acidic pH, reflecting that of the stomach, until reaching the small intestine. Upon dissolution, the fluid is sampled via embedded gratings, and pancreatic lipase reacts with triglyceride coatings to increase the capacitance of the sensors. The signal is transmitted to a phone wirelessly and shared with a medical practitioner.

Materials and Methods

A. Description of Device, Operation, and Data Acquisition

The capsules were designed and assembled at the University of Maryland, College Park. The capsule shell is 3D-printed with MED610, a biocompatible resin, using an Objet500 Connex3 (Stratasys, Rehovot, Israel). The printed circuit board (PCB) and electronic components, were commercially manufactured (Sunstone, Mulino, OR) and assembled (Screaming Circuits, Canby, OR). Specifications for the system electronics and capsule dimensions are presented in Table 1, while a detailed method describing the capsule assembly is discussed in Supplemental Figure S1. The capacitive sensors consist of interdigitated electrodes, described previously, capped with plasma-enhanced chemical vapor deposited 100 nm SiO_2 films (49). Figure 2 depicts photographs of the sensor PCB assembly (SPA), and the subsequent encapsulation in the capsule shell. In commentary of the capsule dimensions, the current largest capsule standard size is 000, which measures at 9.9 mm x 26.1 mm, whereas the dimensions of the clinically utilized InteliSite capsule (Innovative Devices, LLC, Raleigh, North Carolina, USA) measures at 10 mm x 35 mm, indicating larger capsules may still be usable for certain populations (50). Efforts to reduce dimensions are continuously in development to reduce potential for affecting GI motility, while more discussion on current capsule dimensions can be found in other studies (4).

Lab on a chip

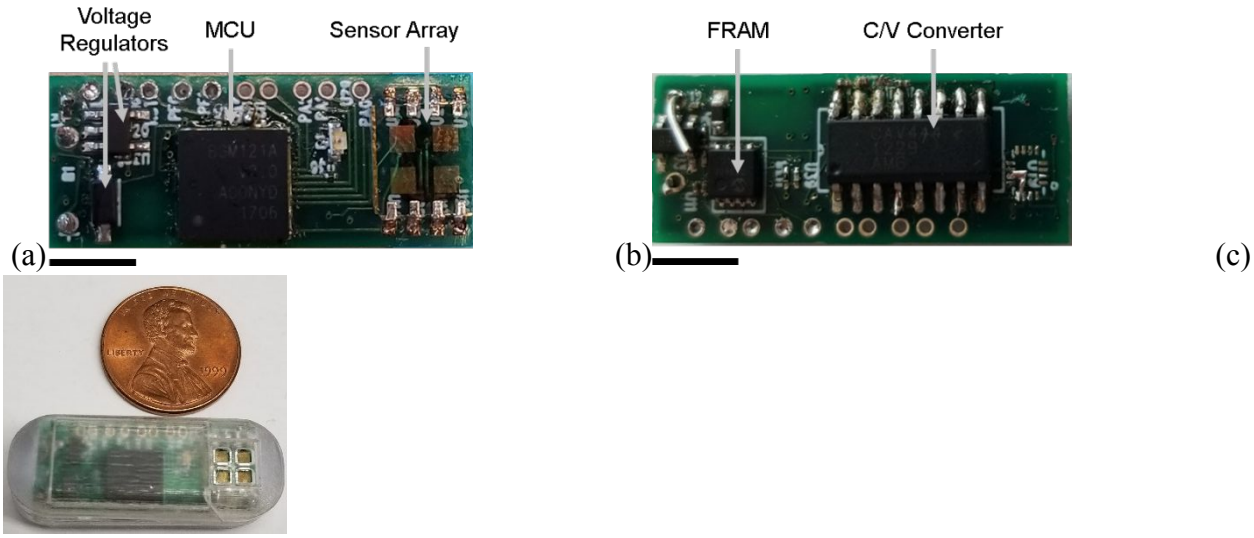

Figure 2: (a) Top and (b) bottom views of sensor PCB assembly (SPA), and (c) photograph of assembled capsule. Scale bar =5 mm.

The SPA was powered at 3.3 V and paired to a nearby Android phone via BLE through a custom application. To operate the device, a signal was transmitted from the phone to trigger the SPA to enter Deep Sleep mode (2.5 µA) for 2.5 hour, allowing for material deposition processes to be completed. Following the Deep Sleep duration, the SPA entered Active mode (~ 5 mA), the app would request a capacitance value from the microcontroller with a sampling rate of 1 Hz. The data is timestamped and stored into a matrix, which could be uploaded to the cloud after each experiment and downloaded to a PC. The data was then visualized for analysis with a MATLAB GUI**.**

3D-Printed Shell	
Outer Diameter	12.7mm
Inner Diameter	11.5 mm
Length	35 mm
Inlet area	4 mm^2
Sensors	
Finger Width	5 µm
Finger Spacing	5 µm
Finger Length	750 µm
Number of Fingers	80
Finger Thickness	200/20 Au/Cr nm

Electronics	
PCB Length	25.8 mm
PCB Width	10.4 mm
Sensor Capacitance Range	0.8-220 pF
Sensor Capacitance Sensitivity	7.3 pF/mV
Operating Voltage	3.3/5.0 V (component dependent)
Current Consumption	Active/Deep Sleep: 5 mA/2.5 µA
Battery (Powerstream)	Li-Polymer/14 mAh/3.7 V
Wireless Communication	BLE 2.4 GHz

Table 1: System specifications.

B. *Deposition of Film and Coating Materials*

The sensing mechanism is based on the enzymatic and physicochemical reactions presented in Figure 3, which features (a) the hydrolysis of triglyceride ester linkages by PL and (b) the emulsification of triglyceride globules by BAs. Stearin was used as a model triglyceride due to its high melting point (54-72.5°C) to remain stable at physiological temperature (37-39°C) (51). The triglyceride solution was prepared for coating onto the sensor surface and consisted of a mixture of stearin and glycerol, where several stearin:glycerol (SG) ratios were evaluated. The combinations included stearin, 2:1, 1:1, and 1:2 ratios of SG after allowing the suspension to melt in a 100°C water bath prior to deposition. Multiple film deposition strategies were investigated, as depicted in Supplemental Figure S2. Drop-casting and dip-coating of molten SG solution, while the substrates were either left at ambient or pre-heated for 5 minutes to SG melting temperature, were compared. In evaluating overall stability and uniformity, the films used for testing PL and BA were deposited via dip-coating of the SPAs, depicted in Figure 4a. The SPAs were pre-heated for 5 minutes to above substrate melting temperature (~100°C), then immersed and subsequently removed The films were air cooled at ambient temperature, forming SG-coated SPAs (SG-SPAs), and the resulting thicknesses were measured using calipers.

The SG-SPAs were inserted into the capsule via the assembly process described in Supplemental Figure S1, and the capsules were subsequently dip-coated into a dyed pH-sensitive copolymer solution, depicted in Figure 4b. The copolymer solution utilized for this study was 30% Eudragit L100 in methanol, producing coatings 783±60 µm thick using a previously described coating process (49). After coating, capsules were stored between 24 and 48 hours before experiments at ambient temperature (~23-24°C), though storage at different temperatures may affect coating stability over time.

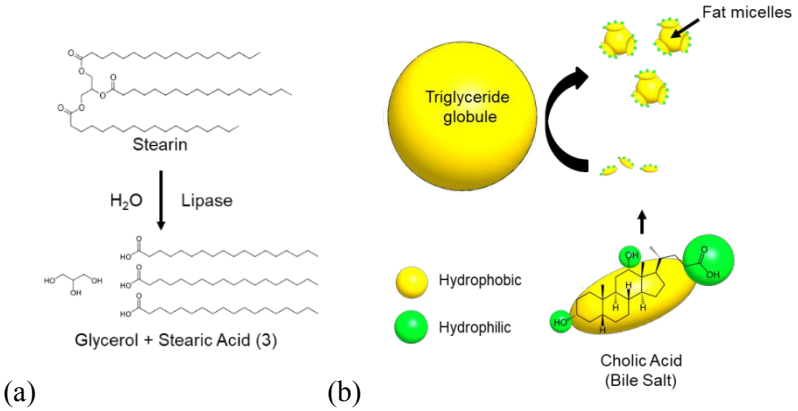

Figure 3: (a) Lipase-induced hydrolytic digestion of stearin into glycerol and three stearic acid molecules. (b) Bile salt-induced emulsification of triglyceride globules into micelles.

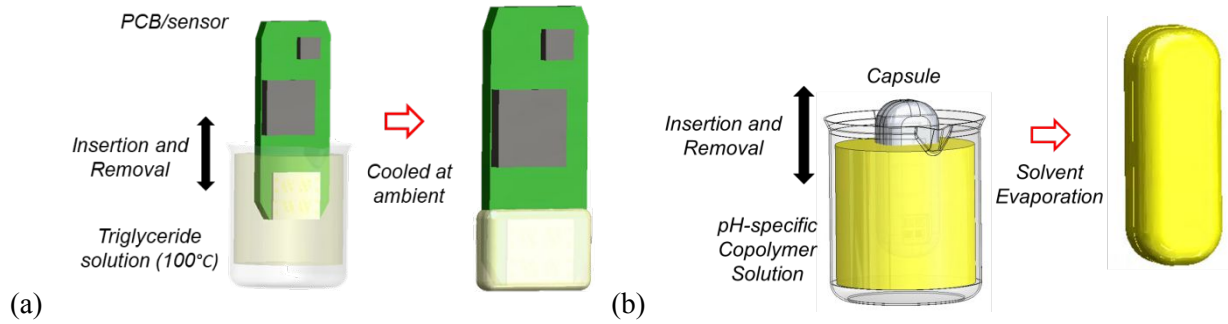

Figure 4: (a) Dip-coating of pre-heated PCB/sensor assemblies into triglyceride solution for film formation. (b) Dip-coating of assembled capsules into dyed pH-sensitive copolymer solutions to form GI-targeting coatings, repeated for sequential coatings.

C. Sensing Characterization

SG-SPA characterization was performed while powered by an Agilent E3631A DC power supply (Santa Clara, CA) . For the SG-SPAs prepared in Section B, each experiment was initiated with baseline measurements while the device was suspended in air. After 5 minutes, the devices were lowered into a 50 mL beaker containing solutions of either negative control – i.e. buffer only – then subsequent test conditions, described below. All buffer solutions consisted of 40 mL of 0.1 M phosphate buffered saline (PBS) on a hot plate set to 300 RPM stir via magnetic stir bar to equilibrate the solution and temperature at 39°C. All solutions were prepared using deionized water from E-pure Ultrapure Water Purification Systems (DI H_2O; resistivity=18.0 Ω-cm; Thermo Scientific, Waltham, MA).

The sensor capacitance response was determined for each analyte in an environment that simulated fluids present in the duodenum. SG-SPAs were immersed in pH 7.3 buffer containing varying concentrations of either porcine PL or a BA mixture of sodium cholate and sodium deoxycholate (Sigma Aldrich, St. Louis, MO). PL was tested at 1 mM, 100 μM, and 10 μM concentrations, while BA was tested across 175, 17.5, and 1.75 mM, equivalent to 7, 0.7, and 0.07 %w/v. To measure potential impact of nonspecific enzymes, porcine pancreatic trypsin (Sigma) was also tested alone at 100 μM, a concentration that exceeds maximum expected outputs by >250 % (52). Each solution was incubated for 30 minutes at 39°C prior to insertion into a beaker for testing the SG-SPAs to ensure complete solubility.

D. SEM Analysis for Film Morphology

Pre-heated sensor die were inserted into molten 2:1 SG solution prepared as described in Section B. The sensors were then cooled at ambient (23°C) for 24 hours, then incubated in glass petri dishes containing PBS (0.1 M) alone or with either 100 μM PL, 0.7 %w/v BA or 100 μM trypsin, respectively. Each solution was maintained at 39°C under 300 rpm stir. Sensors were removed from solution after either 30- or 60-minutes, rinsed with DI H_2O, dried for 24 hours, then prepared in a carbon coater to deposit coatings of conductive carbon (MED 010 Balzers Union Carbon Coater, Balzers Union, Liechtenstein). The samples were then viewed under a Hitachi S-3400 scanning electron microscope (SEM).

E. pH-|Dependent Sampling and Sensing

Following a similar procedure as in Section C, measurements were performed while suspending the coated capsule in air, then subsequently inserted into a test solution. For these experiments, the electronics were powered by a Li-polymer battery (Powerstream, West Orem, Utah). The capsules were inserted for a duration of 25 min into several solutions, which mimicked the pH transition between the stomach (acidic) and duodenum (neutral), as depicted in Figure 5. The solutions consisted of the following conditions: (i) 0.1 M acetic acid (pH 3), (ii) PBS (pH 7.3), and (iii) 1 mM PL in PBS (pH 7.3). This sequence was chosen to reflect the capsule transit throughout the GI tract with the subsequent presence of a specific biomarker residing in the SI, in this case PL.

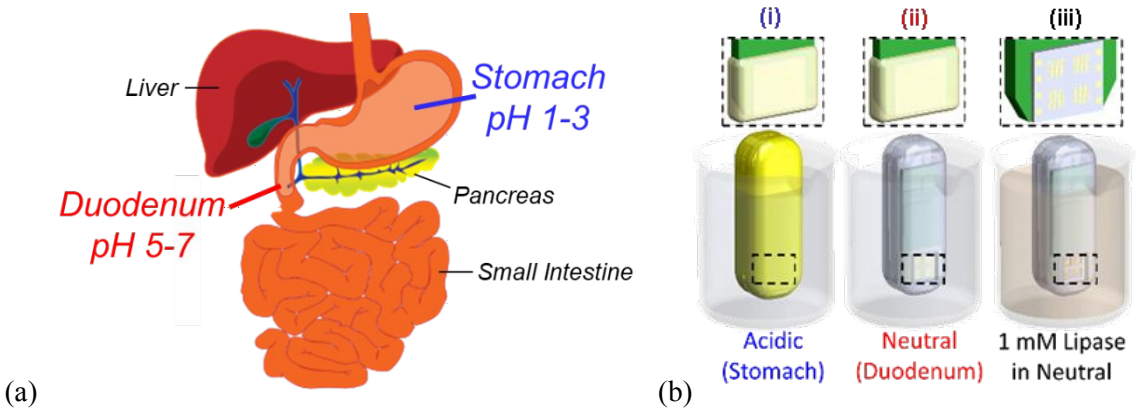

Figure 5: (a) Schematic depicting normal GI pH progression along with adjacent organs. (b) Experimental setup for complete capsule characterization.

Results & Discussion

This work presents a sensing strategy using triglyceride films to detect duodenal contents, such as lipase and bile acids, in a wireless capacitive-sensing platform. The sensors were designed to measure the capacitive response when fluid enters the sensing chamber. Under biological stimuli from species in the environment, the substrate films deposited over the sensors undergo hydrolysis or emulsification reactions that alter their dielectric property. Gradually, the dissolution of the film substrate exposes the electrode fingers to the infiltrating fluid, causing an increase in capacitance. The sensor capacitance was measured for SG-SPAs and coated capsules inserted into various solutions containing biochemical stimuli, described in C and E, which induce changes in capacitance over different lengths of time when compared to non-specific controls or buffer alone.

Stearin was the material chosen as our model triglyceride, as described in B. The digestion of triglycerides, is enabled by emulsion and subsequent hydrolysis by BAs and PL, respectively. Due to its rigidity and low water solubility – an effect of having longer chain fatty acids – unmodified stearin is an inefficient substrate for hydrolysis. Other triglycerides such as oleic acid – a shorter chain fatty acid found in olive oil – are used as standard substrate for lipase assays; however, these substrates are incompatible with our system function in the small intestine due to having a melting point below physiological temperature (53). Previous reports modify stearin as a substrate using suspensions with glycerol by enhancing the quality of the interface it would have with lipase (54–56). Lipase activity on triglycerides is generally dependent on the surface area, which increases significantly with rougher surfaces or when emulsified into micelles by BAs. While crystalline stearin films are naturally hydrophobic, glycerol is hydrophilic due to polar –OH groups, enhancing the interface between the species in solution and the film substrate, as well as a stable film deposition and adhesion over the sensor surfaces.

Because the platform has demonstrated utility for monitoring changes in sensor capacitance (C), the dielectric properties of the films can be described through estimation by equation (1):

$$C = \frac{2\varepsilon_r\varepsilon_0 lwn}{d} = \frac{\varepsilon_r\varepsilon_0 A}{d} \quad (1)$$

Here, ε_0 (vacuum permittivity), ε_r (dielectric constant), l (finger length), w (finger width), n (numbers of electrode fingers), and d (distance of separation), where $2lwn$ can be simplified to A (total area of both electrodes). Therefore, cumulative changes in the dielectric properties and thickness of the films are proportional to measured capacitance (C) and indicate the extent of hydrolysis or emulsification of the substrate over the sensor. To account for changes in baseline capacitance between experiments, the sensor response as the percent change in capacitance (%ΔC) can be calculated with equation (2):

$$\%\Delta C = \left(\frac{C_n - C_1}{C_1}\right) * 100 \quad (2)$$

Here, C_n is the capacitance at n sample in time, where C_1 is the capacitance at the beginning of the recorded sequence such as those presented in Figure 6.

When no film is present – i.e. one of our negative controls – and the sensor is inserted into PBS, the mean %ΔC is 39.5±1.4, likely a resulting effect of the higher dielectric constant of water as compared to air combined with ionic reactions with the SiO_2 films, which can be mitigated in the future through more inert films (57). As expected, insertion into molten and cooled SG solutions produced negligible %ΔC, indicating that changes in capacitance are limited to (when the dielectric properties of the SG material is influenced by an environmental condition – such as the applied solutions and constituent analytes described in C (.

Initial tests consisted of the effect of different deposition strategies of the SG solutions onto the sensors, described in Section B. Substrate temperature was considered a significant factor due to its effect on surface tension, and therefore wetting of the solution (58). In the case of drop-casting, three phases (i.e. solid, liquid, gas) are present at the sensor surface during the entirety of the process, thus surface tension becomes a more dominant factor for wetting, and therefore coating, the sensors. Wetting through dip-coating, however, causes most of the sensor surface (except for the edges) to be exposed to only two phases with the ability for a complete wetting and sealing layer, reducing the dependency on surface tension. Additionally, the order of the wetting transition has a direct impact on the adsorbed film thickness, such that the greater the discontinuity in the interfacial energy between phases, the greater the thickness. This discontinuity is reflected by the difference in temperature between the substrate and film, which were observed through thinner films produced when the substrates are pre-heated. SiO_2 films on the sensor surfaces are generally hydrophilic, with surface energies of ~73.8 mJ/m^2, compared to most triglycerides, which maintain surface energies ranging from 25-30 mJ/m^2 as reported in the literature; this increases with temperature as well, producing further discontinuity and, therefore, wetting angle (59,60). Adhesion between the SiO_2 and SG layers is primarily based on van der Waals interactions; however, the drop-cast films were found to not be stable, as the films did not produce an adequate enough seal at the substrate surface and failed to prevent buffer from interacting with the sensors (data not shown) (61). After comparing the efficacy of the film deposition methods, SG-SPAs were tested using films produced through pre-heating the substrate to 100°C and dip-coating, which yielded an average film thickness of 210±60.3 μm. The total sensor area was 0.06 mm^2, indicating each film volume over the sensors to be 1.25x10^{-5} cm^3. In comparing the sensor response for different SG film compositions (see C), the 2:1 SG ratio films were found to be most stable when in buffer alone (Supplemental Figure S3), hence their implementation in the following sensor characterization experiments. From the 2:1 SG ratio, the volume of stearin contained within the film was calculated to be 0.84x10^{-5} cm^3, and with a density of 0.862 g/cm^3, the stearin mass was found to be 0.724x10^{-5} g, or 8.12x10^{-9} mol (molecular weight of stearin:891.5 g/mol).

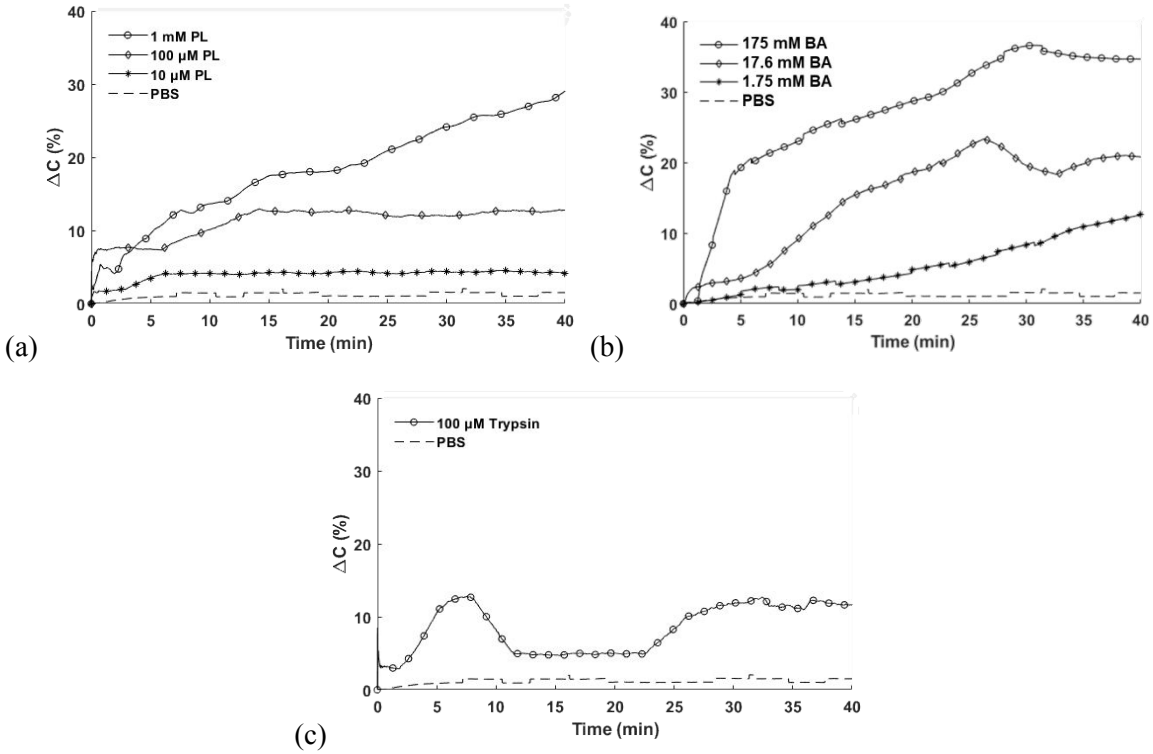

Figure 6: Sensing in the presence of different biochemical species at varying concentrations compared to PBS alone. (a) PL at 10 µM, 100 µM, and 1 mM, (b) BAs at 1.75, 17.5, and 175 mM, and (c) pancreatic trypsin at 100 µM.

The standard concentration of PL expected in healthy unstimulated duodenal fluid ranges from 1-10 µM (62). Conversely, average duodenal secretions contain 0.7 %w/v BA, which reflects the median concentration tested in this work (63). Because PL is dependent on BAs for improving the enzyme-substrate interface with triglycerides, it was necessary to determine the individual effect of both species on the dielectric properties of the film, which can range from characteristics such as ratio of stearic acid to glycerol via hydrolysis, stearin to glycerol through emulsion separation, or even overall SG film to solution contact with the sensor surface. Figure 6 presents the capacitive response (%ΔC) of the SG-SPA over time upon immediate insertion into the solution at t=0 minutes, where the concentration of the biological stimuli was varied for PL (0.01-1 mM) and BAs (1.75-175 mM), as well as pancreatic trypsin (100 µM) to measure potential nonspecific interactions. Each sequence begins directly following insertion of the SG-SPA into the test solution to precede experiments of the sensors within a capsule device. Measurements were compared to a buffer-only solution (7.3 pH, PBS) as a negative control. The capacitance responses of films to both PL and BAs produced trends that altered proportionally to the concentration of the analytes present. Conversely, the signal for trypsin did not produce consistent trends, and appeared to experience stabilizing transients throughout the time frame of the experiments; the effect of trypsin at different concentrations requires further investigation. The measurement was conducted over the course of 40 minutes, consistent with the expected transit time of most contents passing through the duodenum, though longer time scales have been reported (64). Additionally, nonspecific activity testing with extracted duodenal secretions and its regular contents will be necessary for increasing confidence in sensor specificity, though stearin appears to be a resilient insulator to negative controls. To modify the system for response to lower concentrations, it is likely that parameters such as concentration of substrate at the sensor surface or film thickness will need to be reduced such that the dielectric properties of the

film can change faster. This is consistent with our findings where films exceeding 200 μm thickness produced no significant change in capacitance compared to buffer alone (data not shown), indicating that either increasing film thickness may reduce reactivity or penetration of the enzyme or that the film is too thick to see a measurable effect over the experimental time period, requiring more film removal before observing a change in capacitance. Reducing the film thickness would be feasible through closer matching of the surface energies, such as through temperature or surface tension, between the SPAs and SG solution before dip-coating, as well as dissolving the triglyceride in nonpolar solvents such as ethers, hexane, or chloroform in lower concentrations (29,65).

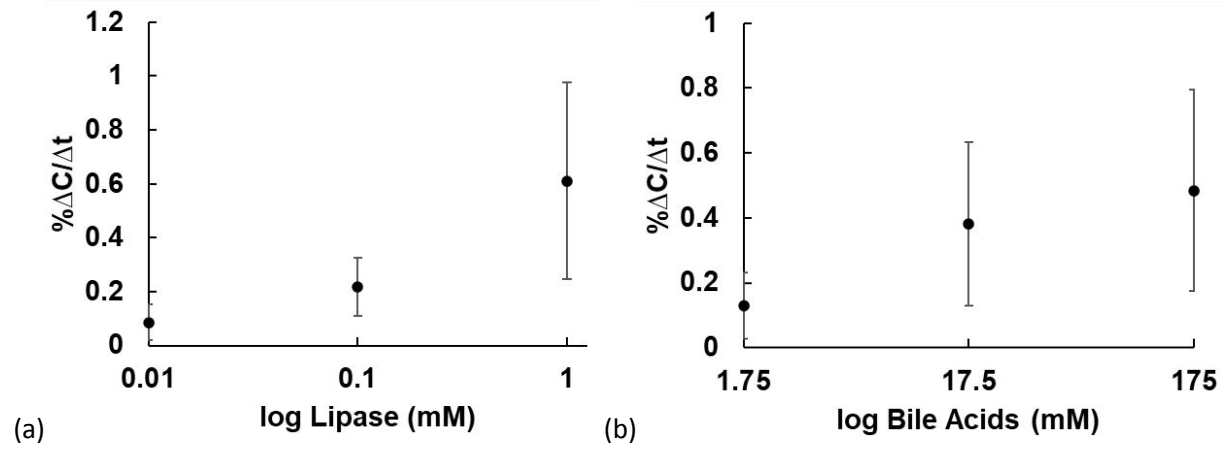

Figure 7: Semi-logarithmic calibration curves of slope responses for 30 min of (a) PL and (b) BAs (n=3).X-axis represents the concentration of the analyte in 40 mL solution under 300 RPM stir at 39°C. Y-axis calculated using %ΔC/ (Δt=30 min). Error bars = standard deviation.

After measuring the capacitive response to each concentration, the slopes were used as a metric to fit the sensitivity. Figure 7 presents calibration curves comparing the slope of the capacitive response for the first 30 minutes of sampling (%ΔC/Δt) compared between concentrations of each analyte at different magnitudes, indicating a positive correlation between analyte concentration and sensor response within the tested ranges. (Statistical analysis was performed, consisting of one-way ANOVA between the three concentrations (α=0.05) for both PL and BA respectively resulting in p-values of 0.12 and 0.17. Unfortunately, the slope of the response at different concentrations appear to lack distinction, as one can see that the error bars overlap significantly. The sensor is essentially two capacitors in series, one made of the SG film and another made using the layer of solution above, consisting mostly of water. As the SG film dissolves or reacts from the analyte, it becomes thinner and the effect of the water capacitor becomes larger as its distance to the sensor diminishes. The time course over which this occurs is dependent on several factors including the film thickness. The up to 55% variation in the starting film thickness could explain some of the overlap between the measured result at these concentrations.

Enzymatic kinetics remain a complex issue, and the lack of difference between the removal time of the films (as indicated by the change in capacitance per time) could indicate that the enzymes or emulsion agents are saturated at the lower concentrations and simply are not able to remove the film at a higher rate. Furthermore, the major effect leading to a change in capacitance with the film dissolution is the replacement of the SG film (which has a relatively low relative dielectric constant of ~15.9) with water having a relative dielectric constant of 80. Another possible effect is differences in the emulsification and hydrolysis reactions where hydrolysis via PL produces glycerol and stearic acid, each of which impact the capacitance of the sensor during the course of the experiment. Alternatively,

emulsification does not alter the material chemical composition, merely the particle size and therefore phase properties of the film, allowing enhanced exposure of the SiO_2 surface of the sensors to constituents in the environmental fluid, even those such as divalent cations (66). However, the fact that the capacitance change curves are similar for the hydrolysis and emulsification reaction indicate that likely in both cases the change in capacitance is likely due to changes in dielectric constant due to water instead of being dominated by the production of an intermediate analyte. Future investigations will need to focus on how to generate a sensor response that is more concentration dependent. Fortunately, a sensor such as the one demonstrated here could find use in GI diagnostic applications where luminal contents are refluxing or failing to be absorbed properly, making it present in a portion of the alimentary canal where it is irritating. Examples of this include bile reflux into the stomach, bile entry into the colon, and acid reflux into the stomach (67,68)

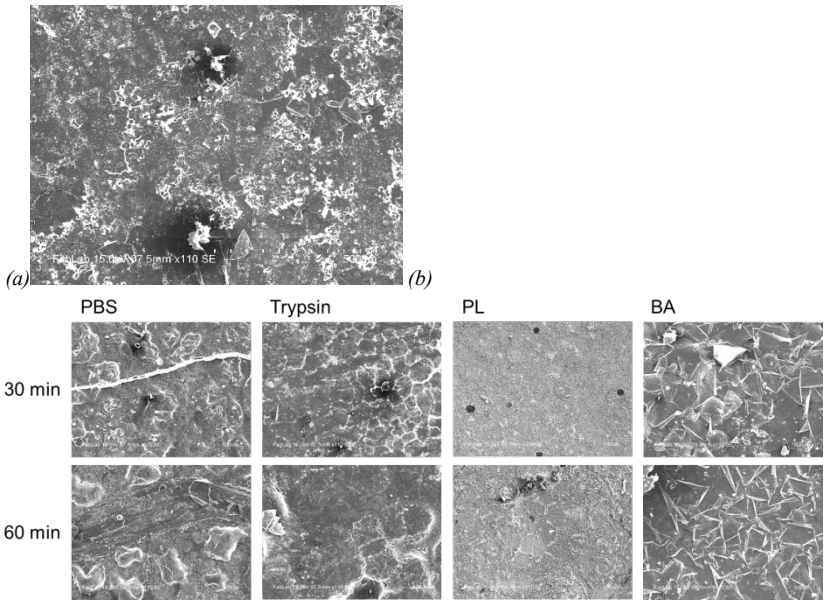

Figure 8: SEM characterization of SG films at (a) 0-minutes and (b) after exposure to various solutions at 30- and 60-minute time intervals.

Morphological differences comparing the impact of each species on the SG films, were viewed under SEM (110x magnification), after deposition of a carbon coating for conductivity. The films had been incubated under stir condition to each solution, and removed at two time points, 30 minutes and 60 minutes, as shown in Figure 8. The 30-minute time point was used to correspond the film morphology to the endpoints of the $\%\Delta C/\Delta T$ values used for Figure 7, while the 60-minute time point was used to determine if any significant changes in the film morphology occurred beyond the used duration. Here, there is little difference between the samples exposed to either PBS or trypsin, whereas the surfaces for PL and BA indicate significant qualitative changes in roughness and crystallization, respectively, though more on crystallization profiles of stearin can be found elsewhere (69). For the PL-exposed sample, the surface appears significantly smoother, likely an effect of the hydrolytic interface occurring between PL and the stearin that reduces surface roughness, and therefore interfacial surface area, until eventual saturation. The BA-exposed sample, however, presents the formation of an increasingly fragmented stearin surface, offering insight as to how hydrolysis and emulsification manifest differently on the substrate. Based on the capacitive changes observed in Figure 6, these structural changes may be direct

indicators for changes in either dielectric properties of the film material or, more likely, changes in film thickness through hydrolytic- or emulsification-induced fragmentation, exposing the surface area of the underlying electrodes to the high-dielectric behavior of the buffer. The lack of significant change between the 30- and 60-minute time points also imply that the durations used for the data in Figure 7 are enough to correspond signal saturation to the morphological state.

Finally, the ability to measure PL within the capsule was tested in benchtop environment that varied the pH overtime and introduced PL at a recorded time point to simulate traveling through the GI tract and detection in the duodenum environment. Figure 9 presents the result of testing the coated capsule containing the SG-SPAs for performing pH-targeted sampling, using the experiments for Figures 6-7 as reference to determine differences in performance when the sensors are outside of or inside the capsule. The respective conditions are labeled as *acid*, *neutral*, and *lipase*, where the capsule was inserted into a pH 3 solution (0.1 M acetic acid) to represent acidic contents for the stomach, pH 7.3 solution (0.1 M PBS) for the duodenum, and addition of PL (1 mM PL in 0.1 M PBS) as a target analyte, respectively. Here, the sensor responses are overlaid for more direct sequence comparison and presented in capacitance rather than %ΔC to show how they compare from beginning to end of each condition. Upon insertion into the *acid* condition, negative drift was observed from ~129.5±0.772 pF, eventually saturating at 115.2±0.759 pF, though no inflow of solution into the capsule was evident through visual inspection and the color of the buffer solution remained clear as indicated in Figure 9b-i (49). After ~19 minutes of incubation in the *neutral* condition (0.1 M PBS), a distinct increase in capacitance to 146.1 pF was observed, before reaching saturation at 127.9±0.433 pF. Additionally, the color of the solution gained a red hue reflective of the Eudragit L100 coating color, as seen in Figure 9b-ii, indicating sample entry. Once the capsule was inserted into the *lipase* condition, there was an immediate effect similar to the capacitance sequences observed in Figure 6a, where there is a rapid increase in capacitance over ~14 minutes to reach 216.0±0.602 pF, or 66.8% increase from the beginning, with some signal fluctuation and decrease as well until it levels around 158.5±0.913 pF, or a 22.4% increase. Due to the opacity of the PL solution, no distinguishable features were discernable until capsule removal, where there is a noticeable region in the Eudragit L100 coating where the fluid could enter the capsule sensing chamber, shown in Figure 9b-iv.

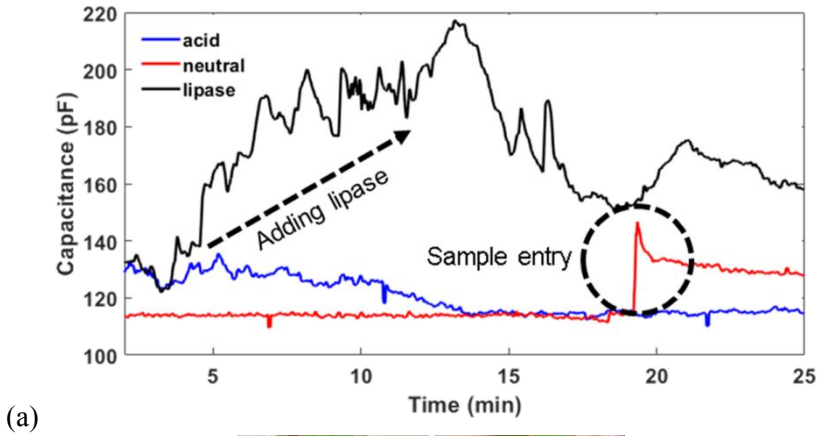

(a) (b)

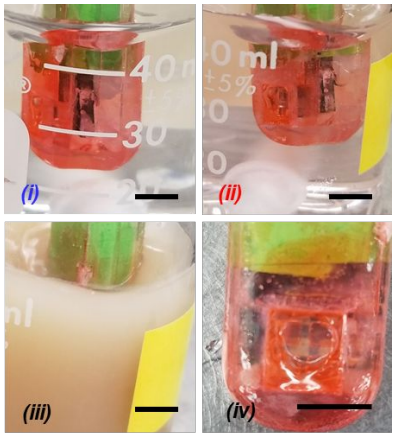

Figure 9: (a) Combined pH sampling and enzyme sensing in integrated capsule. Measurements were initiated after immersion into acidic solution for 25 minutes (blue), after which the capsules were removed and immersed into a neutral solution (red), where a spike was observed around 19 minutes, indicated by the circle. Finally, the capsule was removed and immersed into a solution containing 1 mM lipase (black), where a distinct increase in capacitance is observed, indicated by the arrow. (b) Photographs taken of the capsule at the end of each respective sequence, designated by the label color: b-i: acid *condition, b-ii:* neutral *condition, b-iii:* lipase *condition, and b-iv* lipase *condition after removal from the solution. Scale bar =5 mm.*

The slope from the first 30 minutes of the *lipase* condition was calculated to yield 0.198 pF/min. Comparing the linear fit with that produced in Figure 7a, the slope changes with concentration of PL. This slope is calculated as a ~3-fold loss in sensor response compared to the mean response for 1 mM lipase (0.610±0.364 pF/min) while also outside the error range, indicating potential loss in SG-SPA response to the analyte when packaged within the capsule rather than when tested without it; this is not surprising, though, considering the differences in fluid dynamics and flow profile of the analyte in the sensing chamber as opposed to when the SG-SPA is surrounded by the fluid in the beaker. However, this emphasizes the need to enhance the exposure of the SG-coated sensors to the surrounding environment, which can be implemented by reducing the thickness of the 3D-printed shell at the inlets or by embedding the sensors directly onto the outermost packaging of the capsule. Ultimately, this experiment demonstrated the sequential ability of the capsule package to remain intact in a potential gastric environment, dissolve from duodenal fluids and allow detection of PL in the same environment. Based on the results presented in Figures 6-7, it is likely this similar strategy can be leveraged to detect BAs in

target pH environments as well, in addition to measuring PL or BA related pathologies such as those discussed above.

Conclusion

This work presents a proof-of-concept demonstration of triglyceride-based coatings for monitoring simulated duodenal analytes in an integrated capsule system. The contents consist of preliminary sensor characterization while primarily introducing a system-integrated approach to ingestible device packaging and the potentials for a novel sensing platform for lipase and bile acids. The device discussed in this paper demonstrates the ability to measure and wirelessly transmit changes in capacitance due to both film hydrolysis and emulsification reactions as a result of exposure of stearin films to PL and BAs, respectively. For PL, signals were measurable for 10 μM-1 mM concentrations, whereas signals from BAs were distinguishable between 1.75-175 mM concentrations, each of which are within physiologically relevant ranges for healthy and abnormal levels. For each concentration, the observed slope produced from the first 30 minutes, which is well within the average duration range for material traveling through the human duodenum, was usable to relate the signal to its respective concentration (64). Furthermore, morphological differences were characterized in triglyceride-based films after exposure to various duodenal contents, giving insight as to the physical manifestation of hydrolytic versus emulsification reaction mechanism. Finally, the ability to detect PL after subsequent targeting at a pH-specific environment was demonstrated, and it was found that the design of the sensing chamber and the respective inlets could be thinned to prevent reduction in the reactive interface between the sensor surface and environmental contents.

While sensor characterization was limited to environments that only simulated duodenal fluids in pH and isolated analytes, rather than *in vivo* systems, there remain several limitations to our methods for signal analysis and the platform in general. For example, parametric analyses of slopes over different time intervals may allow for distinguishing between each film response over time, thus producing more sensitive or optimal fitting equations to match the concentration with the $\%\Delta C/\Delta T$. The sensor responses are also likely to increase sensitivity if thinner insulating films can be deposited; this would change the amount of substrate and therefore amount of reaction that needs to occur to increase the rate of change in dielectric mismatch between the film and environmental solution, potential altering resulting concentration range for other GI regions where it may be relevant. Next, each species was tested in isolation, and their simultaneous presence has been shown to reduce efficacy due to non-specific film interactions depending on the material used (28). Therefore, it is critical that future work will focus on characterizing and optimizing the sensor performance over a wider concentration range, adding more non-specific species to determine further reaction specificity, and incorporate additional food-based materials, such as gelatin – substrates for monitoring other types of pancreatic enzymes (28). Additionally, different capsule coating materials could be used toward measuring these species in different GI environments – based on their pH – as well as enhance the exposure of the substrate to materials in the external environment. The coatings can be used to protect and expose different types of biosensors to their target regions, enhancing passive localization strategies while notifying the system user of the exact time of exposure. On a similar note, while stearin has demonstrated the potential utility as a substrate for measuring time dependency of either hydrolytic or emulsification reactions, more control over testing conditions would reduce sources of electrical or environmental noise or impedance sensing could be used to examine additional electrical properties of the films. This includes improving the coating process for producing more consistent SG film thicknesses, improving the starting conditions for each of the sensors.

Further investigation is needed of strategies for imparting control to the system or over environmental features to improve analysis since these systems are directed to function in the GI tract, which is an inherently chaotic environment.

Ultimately, this platform provides opportunities for sensing hydrolytic and emulsification reactions, such as through other enzymes or biologicals similar to the species discussed in this work, along with an innovative packaging strategy toward passive GI targeting in minimally invasive and ingestible diagnostics.

Acknowledgements

This work was supported by the National Science Foundation ECCS Program under Award 1738211. The authors acknowledge the support from the Maryland NanoCenter and its FabLab.

References

1. Beardslee LA, Banis GE, Chu S, Liu S, Chapin AA, Stine JM, et al. Ingestible Sensors and Sensing Systems for Minimally Invasive Diagnosis and Monitoring: The Next Frontier in Minimally Invasive Screening. ACS Sensors. 2020 Mar 20;

2. Kalantar-zadeh K, Ha N, Ou JZ, Berean KJ. Ingestible Sensors. ACS Sensors [Internet]. 2017;2 (4):468–83. Available from: https://doi.org/10.1021/acssensors.7b00045

3. Gonzalez-Guillaumin JL, Sadowski DC, Kaler KVIS, Mintchev MP. Ingestible Capsule for Impedance and pH Monitoring in the Esophagus. IEEE Trans Biomed Eng. 2007;54 (12):2231–6.

4. Basar MR, Malek F, Juni KM, Idris MS, Saleh MIM. Ingestible Wireless Capsule Technology: A Review of Development and Future Indication. Kishk AA, editor. Int J Antennas Propag [Internet]. 2012;2012:807165. Available from: https://doi.org/10.1155/2012/807165

5. Nemeth A, Agardh D, Wurm Johansson G, Thorlacius H, Toth E. Video capsule endoscopy in pediatric patients with Crohn's disease: a single-center experience of 180 procedures. Therap Adv Gastroenterol [Internet]. 2018 [cited 2018 Sep 27];11:1756284818758929. Available from: http://www.ncbi.nlm.nih.gov/pubmed/29531578

6. Friedel D, Modayil R, Stavropoulos S. Colon Capsule Endoscopy: Review and Perspectives. Gastroenterol Res Pract [Internet]. 2016;2016:9643162. Available from: http://www.ncbi.nlm.nih.gov/pmc/articles/PMC5028851/

7. Adler SN, Metzger YC. PillCam COLON capsule endoscopy: recent advances and new insights. Therap Adv Gastroenterol [Internet]. 2011;4 (4):265–8. Available from: http://www.ncbi.nlm.nih.gov/pmc/articles/PMC3131168/

8. Moglia A, Menciassi A, Dario P, Cuschieri A. Capsule endoscopy: progress update and challenges ahead. Nat Rev Gastroenterol Hepatol [Internet]. 2009 Jun 12 [cited 2019 Jan 16];6 (6):353–61. Available from: http://www.nature.com/articles/nrgastro.2009.69

9. Ou JZ, Cottrell JJ, Ha N, Pillai N, Yao CK, Berean KJ, et al. Potential of in vivo real-time gastric gas profiling: a pilot evaluation of heat-stress and modulating dietary cinnamon effect in an animal model. Sci Rep [Internet]. 2016;6:33387. Available from: http://dx.doi.org/10.1038/srep33387

10. Kalantar-zadeh K, Yao CK, Berean KJ, Ha N, Ou JZ, Ward SA, et al. Intestinal Gas Capsules: A Proof-of-Concept Demonstration. Gastroenterology [Internet]. 2015;150 (1):37–9. Available from: http://dx.doi.org/10.1053/j.gastro.2015.07.072

11. Ou JZ, Yao CK, Rotbart A, Muir JG, Gibson PR, Kalantar-zadeh K. Human intestinal gas measurement systems: in vitro fermentation and gas capsules. Trends Biotechnol [Internet]. 2015;33 (4):208–13. Available from: http://www.sciencedirect.com/science/article/pii/S0167779915000256

12. Kalantar-Zadeh K, Berean KJ, Ha N, Chrimes AF, Xu K, Grando D, et al. A human pilot trial of ingestible electronic capsules capable of sensing different gases in the gut. Nat Electron [Internet]. 2018 Jan 8 [cited 2019 Jul 30];1 (1):79–87. Available from: http://www.nature.com/articles/s41928-017-0004-x

13. Van Der Schaar PJ, Dijksman JF, Broekhuizen-De Gast H, Shimizu J, Van Lelyveld N, Zou H, et al. A novel ingestible electronic drug delivery and monitoring device. Gastrointest Endosc [Internet]. 2013;78 (3):520–8. Available from: http://dx.doi.org/10.1016/j.gie.2013.03.170

14. Yu W, Rahimi R, Ochoa M, Pinal R, Ziaie B. A Smart Capsule With GI-Tract-Location-Specific Payload Release. IEEE Trans Biomed Eng [Internet]. 2015 Sep [cited 2018 Sep 19];62 (9):2289–95. Available from: http://ieeexplore.ieee.org/document/7089218/

15. Shi Q, Wang J, Chen D, Chen J. In Vitro and In Vivo characterization of wireless and passive micro system enabling gastrointestinal pressure monitoring. 2014;859–68.

16. Arefin MS, Redoute J-M, Yuce MR. Integration of Low-Power ASIC and MEMS Sensors for Monitoring Gastrointestinal Tract Using a Wireless Capsule System. IEEE J Biomed Heal Informatics [Internet]. 2016 Jan [cited 2018 Sep 19];22 (1):87–97. Available from: http://ieeexplore.ieee.org/document/7891895/

17. Demosthenous P, Georgiou J. An ingestible, NIR-fluorometric, cancer-screening capsule. In: 2015 37th Annual International Conference of the IEEE Engineering in Medicine and Biology Society (EMBC) [Internet]. IEEE; 2015 [cited 2018 Sep 19]. p. 2143–6. Available from: http://ieeexplore.ieee.org/document/7318813/

18. Nemiroski A, Ryou M, Thompson C, Westervelt R. Swallowable Fluorometric Capsule for Wireless Triage of Gastrointestinal Bleeding. Lab Chip [Internet]. 2015;15:4479–87. Available from: http://pubs.rsc.org/en/Content/ArticleLanding/2015/LC/C5LC00770D

19. Mimee M, Nadeau P, Hayward A, Carim S, Flanagan S, Jerger L, et al. An ingestible bacterial-electronic system to monitor gastrointestinal health. Science [Internet]. 2018 May 25 [cited 2018 Sep 19];360 (6391):915–8. Available from: http://www.ncbi.nlm.nih.gov/pubmed/29798884

20. van Putten AFP. Electronic Measurement Systems [Internet]. Routledge; 2019 [cited 2019 Aug 2]. Available from: https://www.taylorfrancis.com/books/9781351453141

21. Said HM, Ghishan FK. Physiology of the gastrointestinal tract. 24 p.

22. Chan HN, Tan MJA, Wu H. Point-of-care testing: applications of 3D printing. Lab Chip [Internet]. 2017; Available from: http://dx.doi.org/10.1039/C7LC00397H

23. Tappa K, Jammalamadaka U. Novel Biomaterials Used in Medical 3D Printing Techniques. J Funct Biomater [Internet]. 2018 Feb 7;9 (1):17. Available from: https://www.ncbi.nlm.nih.gov/pubmed/29414913

24. Chia HN, Wu BM. Recent advances in 3D printing of biomaterials. J Biol Eng [Internet]. 2015 Jul

5;9:4. Available from: https://doi.org/10.1186/s13036-015-0001-4

25. Jamróz W, Szafraniec J, Kurek M, Jachowicz R. 3D Printing in Pharmaceutical and Medical Applications - Recent Achievements and Challenges. Pharm Res [Internet]. 2018 Jul 11;35 (9):176. Available from: https://www.ncbi.nlm.nih.gov/pubmed/29998405

26. Sochol RD, Sweet E, Glick CC, Wu S-Y, Yang C, Restaino M, et al. 3D printed microfluidics and microelectronics. Microelectron Eng [Internet]. 2018 Apr 5 [cited 2019 Jan 16];189:52–68. Available from: https://www.sciencedirect.com/science/article/pii/S0167931717304070

27. Xu W, Yang H, Zeng W, Houghton T, Wang X, Murthy R, et al. Food-Based Edible and Nutritive Electronics. Adv Mater Technol [Internet]. 2017 Nov 1 [cited 2019 Jan 16];2 (11):1700181. Available from: http://doi.wiley.com/10.1002/admt.201700181

28. Banis G, Beardslee AL, Ghodssi R. Gelatin-Enabled Microsensor for Pancreatic Trypsin Sensing. Appl Sci. 2018;8 (2).

29. Stoytcheva M, Zlatev R, Velkova Z, Montero G. Nanoparticle modified QCM-based sensor for lipase activity determination. Anal Methods [Internet]. 2013;5 (16):3811–5. Available from: http://dx.doi.org/10.1039/C3AY41047A

30. Stoytcheva M, Zlatev R, Cosnier S, Arredondo M, Valdez B. High sensitive trypsin activity evaluation applying a nanostructured QCM-sensor. Biosens Bioelectron [Internet]. 2013;41 (1):862–6. Available from: http://dx.doi.org/10.1016/j.bios.2012.08.039

31. Kim J, Jeerapan I, Ciui B, Hartel MC, Martin A, Wang J. Edible Electrochemistry: Food Materials Based Electrochemical Sensors. Adv Healthc Mater [Internet]. 2017 Nov 1 [cited 2019 Jan 16];6 (22):1700770. Available from: http://doi.wiley.com/10.1002/adhm.201700770

32. Pandol SJ. The Exocrine Pancreas. Morgan Claypool Life Sci [Internet]. 2010; Available from: https://www.ncbi.nlm.nih.gov/books/NBK54128/

33. Koziolek M, Grimm M, Becker D, Iordanov V, Zou H, Shimizu J, et al. Investigation of pH and Temperature Profiles in the GI Tract of Fasted Human Subjects Using the Intellicap® System. J Pharm Sci [Internet]. 2015;104 (9):2855–63. Available from: http://www.sciencedirect.com/science/article/pii/S002235491630065X

34. Banis GE, Beardslee LA, Stine JM, Sathyam RM, Ghodssi R. Gastrointestinal Targeted Sampling and Sensing via Embedded Packaging of Integrated Capsule System. J Microelectromechanical Syst [Internet]. 2019 [cited 2019 Feb 21];1–7. Available from: https://ieeexplore.ieee.org/document/8643033/

35. Cole ET, Scott RA, Connor AL, Wilding IR, Petereit HU, Schminke C, et al. Enteric coated HPMC capsules designed to achieve intestinal targeting. Int J Pharm. 2002;231 (1):83–95.

36. Ruiz-Valdepeñas Montiel V, Sempionatto JR, Esteban-Fernández de Ávila B, Whitworth A, Campuzano S, Pingarrón JM, et al. Delayed Sensor Activation Based on Transient Coatings: Biofouling Protection in Complex Biofluids. J Am Chem Soc [Internet]. 2018 Oct 31 [cited 2019 Jan 17];140 (43):14050–3. Available from: http://pubs.acs.org/doi/10.1021/jacs.8b08894

37. Ruiz-Valdepeñas Montiel V, Sempionatto JR, Campuzano S, Pingarrón JM, Esteban Fernández de Ávila B, Wang J. Direct electrochemical biosensing in gastrointestinal fluids. Anal Bioanal Chem [Internet]. 2018 Dec 14 [cited 2019 Jan 17];1–8. Available from: http://link.springer.com/10.1007/s00216-018-1528-2

38. Haupt ME, Kwasny MJ, Schechter MS, McColley SA. Pancreatic Enzyme Replacement Therapy

Dosing and Nutritional Outcomes in Children with Cystic Fibrosis. J Pediatr [Internet]. 2014;164 (5):1110-1115.e1. Available from: http://www.sciencedirect.com/science/article/pii/S0022347614000286

39. Harada H, Ono A, Yamamoto N, Ikubo I, Negron A, Hayashi T, et al. Studies on Human Pure Pancreatic Juice Collected by Endoscopic Retrograde Catheterization of the Papilla. Gastroentrologia Jpn. 1978;13 (5):383–9.

40. Ulleberg EK, Comi I, Holm H, Herud EB, Jacobsen M, Vegarud GE. Human Gastrointestinal Juices Intended for Use in In Vitro Digestion Models. Food Dig [Internet]. 2011;2 (1–3):52–61. Available from: http://www.ncbi.nlm.nih.gov/pmc/articles/PMC3339592/

41. Goldberg DM, Wormsley KG. The interrelationships of pancreatic enzymes in human duodenal aspirate. Gut [Internet]. 1970;11 (10):859–66. Available from: http://www.ncbi.nlm.nih.gov/pmc/articles/PMC1553158/

42. Raimondo M, Imoto M, Dimagno EP. Rapid endoscopic secretin stimulation test and discrimination of chronic pancreatitis and pancreatic cancer from disease controls. Clin Gastroenterol Hepatol [Internet]. 2003;1 (5):397–403. Available from: http://www.sciencedirect.com/science/article/pii/S1542356503001824

43. Lipase [Internet]. [cited 2019 Jan 16]. Available from: https://labtestsonline.org/tests/lipase

44. Kost GJ. Guidelines for point-of-care testing. Improving patient outcomes. Am J Clin Pathol [Internet]. 1995 Oct [cited 2019 Jul 22];104 (4 Suppl 1):S111-27. Available from: http://www.ncbi.nlm.nih.gov/pubmed/7484942

45. Vijayvargiya P, Camilleri M, Shin A, Saenger A. Methods for diagnosis of bile acid malabsorption in clinical practice. Clin Gastroenterol Hepatol [Internet]. 2013 Oct [cited 2019 Apr 29];11 (10):1232–9. Available from: http://www.ncbi.nlm.nih.gov/pubmed/23644387

46. Degirolamo C, Modica S, Palasciano G, Moschetta A. Bile acids and colon cancer: Solving the puzzle with nuclear receptors. Trends Mol Med [Internet]. 2011 Oct 1 [cited 2019 Apr 29];17 (10):564–72. Available from: https://www.sciencedirect.com/science/article/pii/S1471491411000979?via%3Dihub#bib0190

47. Cheng K, Raufman J-P. Bile acid-induced proliferation of a human colon cancer cell line is mediated by transactivation of epidermal growth factor receptors. Biochem Pharmacol [Internet]. 2005 Oct 1 [cited 2019 Apr 29];70 (7):1035–47. Available from: https://www.sciencedirect.com/science/article/pii/S0006295205004612

48. WEDLAKE L, A'HERN R, RUSSELL D, THOMAS K, WALTERS JRF, ANDREYEV HJN. Systematic review: the prevalence of idiopathic bile acid malabsorption as diagnosed by SeHCAT scanning in patients with diarrhoea-predominant irritable bowel syndrome. Aliment Pharmacol Ther [Internet]. 2009 Oct 1 [cited 2019 Apr 29];30 (7):707–17. Available from: http://doi.wiley.com/10.1111/j.1365-2036.2009.04081.x

49. Banis GE, Member S, Beardslee LA, Stine JM, Sathyam RM, Ghodssi R. Gastrointestinal Targeted Sampling and Sensing via Embedded Packaging of Integrated Capsule System. J Microelectromechanical Syst. 2019;PP:1–7.

50. Koulaouzidis A. Wireless endoscopy in 2020: Will it still be a capsule? World J Gastroenterol [Internet]. 2015 [cited 2018 Sep 19];21 (17):5119. Available from: http://www.wjgnet.com/1007-9327/full/v21/i17/5119.htm

51. Charbonnet GH, Singleton WS. Thermal properties of fats and oils. J Am Oil Chem Soc [Internet].

1947 May 1 [cited 2019 Jan 18];24 (5):140–2. Available from: http://doi.wiley.com/10.1007/BF02643296

52. Lake-Bakaar G, McKavanagh S, Rubio CE, Epstein O, Summerfield JA. Measurement of trypsin in duodenal juice by radioimmunoassay. Gut [Internet]. 1980 May [cited 2019 Jun 20];21 (5):402–7. Available from: http://www.ncbi.nlm.nih.gov/pubmed/7429303

53. American Chemical Society. Reagent chemicals : American Chemical Society specifications, official from April 1, 1993. The Society; 1993. 806 p.

54. American Society of Biological Chemists., Rockefeller Institute for Medical Research., American Society for Biochemistry and Molecular Biology. The Journal of biological chemistry. [Internet]. American Society for Biochemistry and Molecular Biology; [cited 2019 Jan 18]. Available from: http://www.jbc.org/cgi/framedreprint/123/3/679

55. Robles Medina A, Esteban Cerdán L, Giménez Giménez A, Camacho Páez B, Ibáñez González MJ, Molina Grima E. Lipase-catalyzed esterification of glycerol and polyunsaturated fatty acids from fish and microalgae oils. J Biotechnol [Internet]. 1999 Apr 30 [cited 2018 Nov 9];70 (1–3):379–91. Available from: https://www.sciencedirect.com/science/article/pii/S0168165699000917

56. Speranza P, Ribeiro APB, Macedo GA. Lipase catalyzed interesterification of Amazonian patauá oil and palm stearin for preparation of specific-structured oils. J Food Sci Technol [Internet]. 2015 Dec [cited 2018 Nov 9];52 (12):8268–75. Available from: http://www.ncbi.nlm.nih.gov/pubmed/26604403

57. Lee YK, Yu KJ, Kim Y, Yoon Y, Xie Z, Song E, et al. Kinetics and Chemistry of Hydrolysis of Ultrathin, Thermally Grown Layers of Silicon Oxide as Biofluid Barriers in Flexible Electronic Systems. ACS Appl Mater Interfaces [Internet]. 2017 Dec 13 [cited 2019 Jun 30];9 (49):42633–8. Available from: http://pubs.acs.org/doi/10.1021/acsami.7b15302

58. Bonn D. Wetting transitions. Curr Opin Colloid Interface Sci [Internet]. 2001 Feb 1 [cited 2019 May 14];6 (1):22–7. Available from: https://www.sciencedirect.com/science/article/pii/S1359029400000832

59. Michalski M-C, Saramago BJV. Static and Dynamic Wetting Behavior of Triglycerides on Solid Surfaces. J Colloid Interface Sci [Internet]. 2000 Jul 15 [cited 2019 May 15];227 (2):380–9. Available from: https://www.sciencedirect.com/science/article/pii/S0021979700968693?via%3Dihub

60. Chumpitaz LDA, Coutinho LF, Meirelles AJA. Surface tension of fatty acids and triglycerides. J Am Oil Chem Soc [Internet]. 1999 Mar [cited 2019 May 15];76 (3):379–82. Available from: http://doi.wiley.com/10.1007/s11746-999-0245-6

61. Xie W, Lewis WM, Kaser J, Ross Welch C, Li P, Nelson CA, et al. Design and Validation of a Biosensor Implantation Capsule Robot. J Biomech Eng [Internet]. 2017 Jun 7 [cited 2019 Jul 14];139 (8):081003. Available from: http://biomechanical.asmedigitalcollection.asme.org/article.aspx?doi=10.1115/1.4036607

62. Carrère J, Galabert C, Thouvenot JP, Figarella C. Assay of human pancreatic lipase in biological fluids using a non-competitive enzyme immunoassay. Clin Chim Acta [Internet]. 1986 Dec 15 [cited 2019 Jun 23];161 (2):209–19. Available from: http://www.ncbi.nlm.nih.gov/pubmed/3542306

63. Barrett KE, Ganong WF. Ganong's review of medical physiology. LK -

https://umaryland.on.worldcat.org/oclc/779244271 [Internet]. 24th ed. /. Lange medical book TA - TT -. New York: McGraw-Hill Medical ; 2012. Available from: http://accesspharmacy.mhmedical.com/book.aspx?bookid=393

64. Camilleri M, Colemont LJ, Phillips SF, Brown ML, Thomforde GM, Chapman N, et al. Human gastric emptying and colonic filling of solids characterized by a new method. Am J Physiol - Gastrointest Liver Physiol. 1989;257 (2).

65. Huang Z, Yu T, Guo L, Lin Z, Zhao Z, Shen Y, et al. Effects of triglycerides levels in human whole blood on the extraction of 19 commonly used drugs using liquid-liquid extraction and gas chromatography-mass spectrometry. Toxicol reports [Internet]. 2015 [cited 2019 Jul 2];2:785–91. Available from: http://www.ncbi.nlm.nih.gov/pubmed/28962414

66. Lee YK, Yu KJ, Kim Y, Yoon Y, Xie Z, Song E, et al. Kinetics and Chemistry of Hydrolysis of Ultrathin, Thermally Grown Layers of Silicon Oxide as Biofluid Barriers in Flexible Electronic Systems. ACS Appl Mater Interfaces [Internet]. 2017 Dec 13 [cited 2019 Jul 4];9 (49):42633–8. Available from: http://pubs.acs.org/doi/10.1021/acsami.7b15302

67. Marin JJG, Macias RIR, Briz O, Monte JMB and MJ. Bile Acids in Physiology, Pathology and Pharmacology [Internet]. Vol. 17, Current Drug Metabolism. 2016. p. 4–29. Available from: http://www.eurekaselect.com/node/136443/article

68. Kauer WKH, Stein HJ. Bile Reflux in the Constellation of Gastroesophageal Reflux Disease. Thorac Surg Clin [Internet]. 2005;15 (3):335–40. Available from: http://www.sciencedirect.com/science/article/pii/S1547412705000186

69. Jiao W, Li L, Yu A, Zhao D, Sheng B, Aikelamu M, et al. In Vitro Gastrointestinal Digestibility of Crystalline Oil-in-Water Emulsions: Influence of Fat Crystal Structure. J Agric Food Chem [Internet]. 2019 Jan 23;67 (3):927–34. Available from: https://doi.org/10.1021/acs.jafc.8b04287

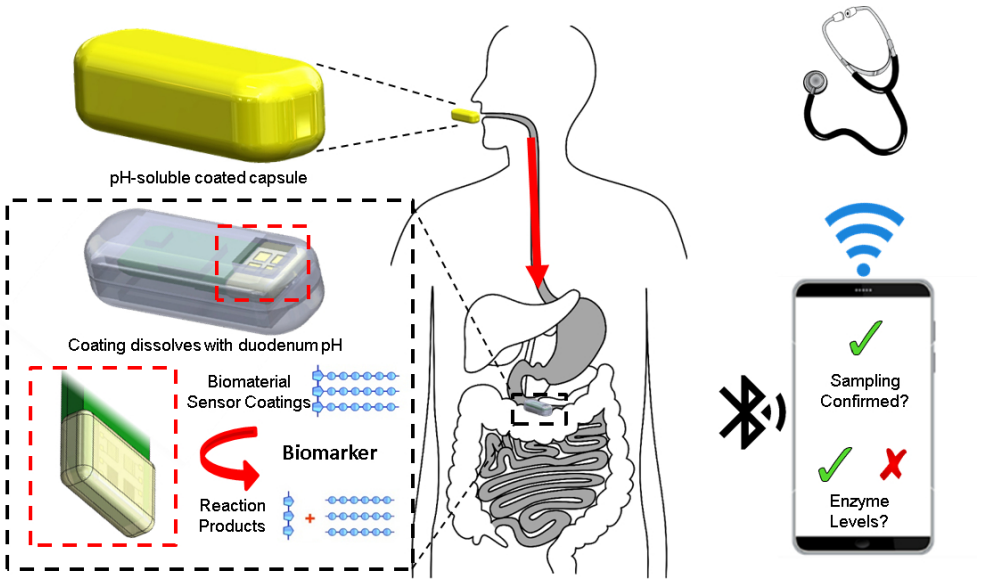

191x109mm (149 x 149 DPI)